

## Direct evidence for the nature of core-level photoemission satellites using angle-resolved photoemission extended fine structure

Edward J. Moler, Scot A. Kellar, Zahid Hussain, Yufeng Chen, and David A. Shirley  
*Advanced Light Source, Lawrence Berkeley National Laboratory, 1 Cyclotron Road, Berkeley, California 94720*

W. R. A. Huff

*Research Center for Spectrochemistry, The University of Tokyo, Photon Factory, National Laboratory for High Energy Physics, Oho 1-1, Tsukuba, Ibaraki 305, Japan*

Zhengqing Huang

*Department of Chemistry and The James Franck Institute, The University of Chicago, Chicago, Illinois 60637*

(Received 18 August 1997)

Photoemission satellites from several systems have been found to exhibit exactly the same angle-resolved photoemission extended fine structure (ARPEFS) as found in the main peaks, when referred to the equivalent photoelectron wave number  $k$  for their own photoelectrons. This provides a direct and powerful method for experimentally determining the angular momentum parameters and the intrinsic/extrinsic nature of core-level photoemission satellites. We present ARPEFS satellite data for nitrogen  $1s$  line in  $c(2 \times 2)$   $N_2/Ni(100)$ , the nickel  $3p$  line in clean nickel (111), the carbon  $1s$  lines in  $(\sqrt{3} \times \sqrt{3})R30$   $CO/Cu(111)$  and  $p2mg(2 \times 1)CO/Ni(110)$ , and the cobalt  $1s$  line in  $p(1 \times 1)$   $Co/Cu(100)$ . For the last two cases the "satellite" structure is actually the low-energy tail of a Doniach-Sunjic line shape. The satellite peaks and the tails of the Doniach-Sunjic line shapes exhibit ARPEFS curves that in all cases except one indicate angular-momentum parameters identical to the main peak and an intrinsic nature. [S0163-1829(97)03648-5]

### I. INTRODUCTION

The nature of core-level photoemission satellites from clean metal surfaces has been an active area of investigation for some time.<sup>1-13</sup> Satellites from molecular adsorbates on metal surfaces have been interpreted as arising from certain mechanisms and employed to study the adsorbate-substrate surface chemical bonds in a variety of systems.<sup>14-20</sup> Core-level satellites are generally described as arising from photoelectron transitions from the neutral ground state to "correlation states" of some type: states lying above the main hole state. Correlation states can be understood as being formed from the main hole states by correlated excitations of valence electrons into unoccupied bound states or into the continuum.

These excitations are often described as a "shakeup" of the valence electrons to form a valence electron-hole pair. However, the satellite peaks in the photoelectron spectrum are produced directly by one-step photoelectron transitions no different from those to the main-peak states. The satellite is "intrinsic" in that it arises from a process that occurs largely within the source atom, leading directly to a final state with the same symmetry as the main hole state, but just lying higher in energy. Indeed, the shakeup picture, per se, while of heuristic value, is unnecessary: the main photoelectron peak and some subset of the intrinsic satellites can be regarded as being formed by transitions from the ground state to a correlated manifold of states of the same symmetry.

In this paper we present a rather stringent test of the above description of correlation satellites. If indeed the satellite peaks associated with core holes, and the low-energy tails accompanying photoelectron peaks in metallic systems,

arise from transitions in which the photoelectron waves originate at the same source atom and are described by the same (bound and continuum) angular momenta as those of the main peak, then they should display the same diffraction phenomena.

Energy-dependent photoelectron diffraction, which we have termed angle-resolved photoemission extended fine structure (ARPEFS), to emphasize its formal similarity to EXAFS when it is observed over a large enough energy range to be analyzed by Fourier-transform methods, provides a very sensitive test of the inherent nature of intrinsic satellites.<sup>21</sup> The scattering phenomena underlying ARPEFS structure are implicitly dependent on the photoelectron wave originating at a precisely located source atom, on its carrying certain angular momenta, and on specific interference phenomena as it scatters from neighboring atoms and propagates to the detector. In the ideal, seemingly simplistic case that a particular satellite line in the photoelectron spectrum arises from a simple photoelectron transition to a higher-energy final state in the same correlation-state manifold as the main-line final state, the satellite's ARPEFS structure should exhibit *exactly* the same variation of intensity with energy as the main line, after correction to the same kinetic-energy scale.

In this paper we examine the ARPEFS structures of several satellite lines that we have observed in our laboratory during studies of surface systems for which the primary goal was the determination of high-accuracy<sup>22</sup> surface atomic structures. When we observed in the course of these studies that the satellite structures also showed ARPEFS oscillations, we elected to combine the analyses of these satellite oscillations and report them together, in this paper. In each

case the satellite ARPEFS structure is compared directly with that of the main line, plotting each intensity against the actual  $k$  value of the photoelectron emitted in the process leading to the main line or the satellite structure. Thus, for a given spectrum, the satellite peak will correspond to a lower  $k$  value than that of the main peak. Section II summarizes the experimental conditions for these systems: more detailed descriptions are given (for most cases) in the publications describing the atomic surface structural determinations. Data reduction is described in Sec. III, and results are given and discussed in Sec. IV. In Sec. V we draw a few conclusions.

## II. EXPERIMENT

Full descriptions of the experimental conditions have been given in reports of the atomic surface structures for both CO/Cu(111) (Ref. 23) and N<sub>2</sub>/Ni(100).<sup>24</sup> For CO/Ni(110), experimental details were given in the structure paper.<sup>25</sup> The Co/Cu(100) work, which has not been published, was studied at room temperature using beam line 6-2 at the Stanford Synchrotron Radiation Laboratory (SSRL). While the exact structure was not determined, cobalt is known to grow layer-by-layer epitaxially on copper (100).<sup>26,27</sup>

The CO/Cu(111) experiment was performed on beam line 9.3.2 at the Advanced Light Source (ALS) at Lawrence Berkeley National Laboratory. The N<sub>2</sub>/Ni(100) experiment was performed on beam line 6.1 at SSRL. The clean nickel and CO/Ni(110) experiments were performed using beam line U3-C at the National Synchrotron Light Source at Brookhaven National Laboratory.

The samples were all cleaned and prepared using standard UHV surface-science techniques and were cooled to 80 K to 120 K for the molecular adsorbates and clean nickel experiments. The x-ray angle of incidence on the sample ranged from 55° to 80° from normal and the emission direction was near-normal for all experiments. We were careful not to radiation damage the adsorbate systems by checking the LEED pattern only briefly near the edge of the sample. It is known that the nitrogen molecule stands on end atop a nickel atom on the (100) surface,<sup>28</sup> and the structure is known.<sup>24</sup> Similarly, the CO is known to occupy only atop sites in the  $(\sqrt{3} \times \sqrt{3})R30$  structure on Cu(111), from FT-IR and EELS (Ref. 29) and, most recently, ARPEFS.<sup>23</sup> The CO molecule in  $p2mg(2 \times 1)$  CO/Ni(110) occupies a displaced, short-bridge site and is tilted by 19° from the surface normal.<sup>25</sup>

## III. DATA REDUCTION

An example x-ray photoemission (XPS) spectrum for each system is shown in Figs. 1, 2, and 3, with the experimental data points shown as circles. The best-fit curves and fitting components are also shown in Figs. 1 and 3. These fits were used to extract the peak intensities for the ARPEFS curves. The range of integration for each spectrum in Fig. 2 is marked by vertical solid lines. The integrated intensities above the background in these regions were used to construct the ARPEFS curves, shown on the right. The abscissa in this plot is the electron wave number  $k$ , in  $\text{\AA}^{-1}$ , for each peak.

The main N 1s XPS peak is known to consist of two components, each associated with the nitrogen closer or far-

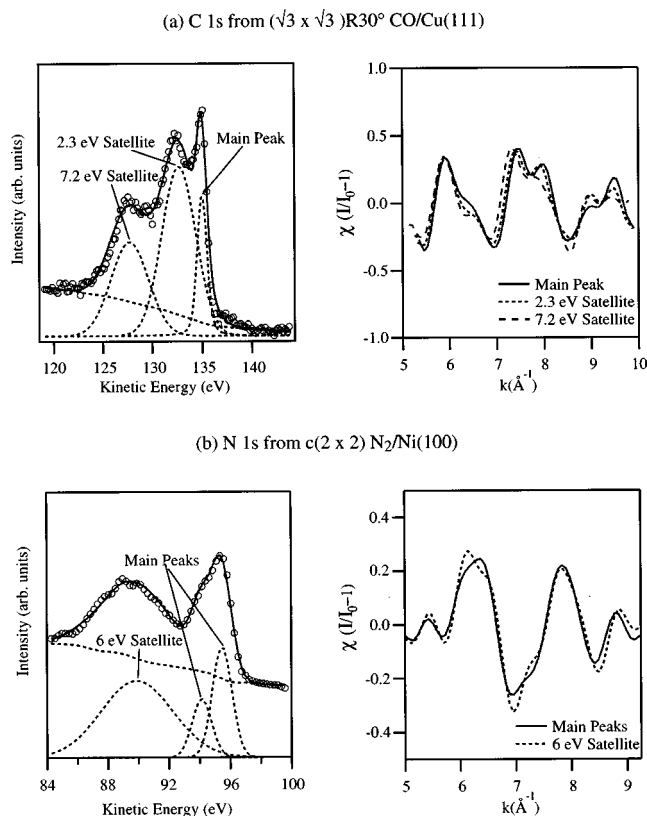


FIG. 1. XPS spectra and ARPEFS  $\chi$  curves for (a)  $(\sqrt{3} \times \sqrt{3})R30$  CO/Cu(111) of the carbon 1s, and (b)  $c(2 \times 2)$  N<sub>2</sub>/Ni(100) of the N 1s core level. The circles in the XPS spectra (left) represent experimental data and the solid curve is the best fit using the components shown in dashes. The peaks were fitted with Voigt functions to extract their intensities. The ARPEFS curve for each peak is shown on the right. Each curve is plotted against the  $k$  value of the photoelectron associated with its corresponding peak. The two main peaks in (b) are summed and the  $k$  value used for plotting the ARPEFS curve is the mean of the two.

ther from the nickel surface.<sup>17</sup> We have summed them to get a sum ARPEFS curve. The nickel  $3p_{1/2}$  and  $3p_{3/2}$  peaks were similarly summed. The C 1s XPS peak in  $p2mg(2 \times 1)$  CO/Ni(110) has been shown to have a Doniach-Sunjc (DS) line shape.<sup>25,30</sup> The cobalt 1s peak in  $p(1 \times 1)$  Co/Cu(100) also shows the Doniach-Sunjc line shape. We have extracted the intensities for these spectra by integrating the area above the background across two regions, one centered on the peak and the other at 10 eV lower kinetic energy, as shown with vertical lines. It is clear from the figures that the satellite peaks exhibit the same ARPEFS diffraction pattern as the main peak, with the exception of the nickel 13-eV satellite, which will be discussed further below. The ARPEFS curves for the  $p2mg(2 \times 1)$  CO/Ni(110) and  $p(1 \times 1)$  Co/Cu(100) systems have been Fourier smoothed to 10  $\text{\AA}$  to aid comparison.

## IV. RESULTS AND DISCUSSION

Two important conclusions, which are related but separate, can be drawn from the similarities between the main- and the satellite-peak ARPEFS curves. The first is that these satellite peaks and the Doniach-Sunjc tails in the photoemission spectrum must arise from “intrinsic” energy-loss

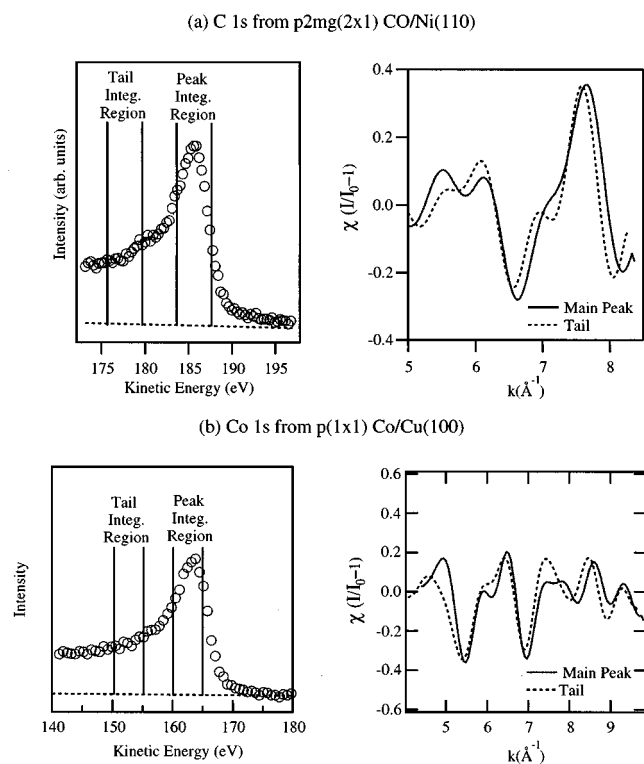


FIG. 2. XPS and ARPEFS curves of (a)  $p2mg(2 \times 1)$  CO/Ni(110), of the carbon 1s core level, and (b)  $p(1 \times 1)$  Co/Cu(100) of the cobalt 1s. The circles in the XPS spectra (left) represent data and the dashes indicate the background component of the spectra. The peak and tail intensities were extracted by numerical integration within the ranges indicated by solid, vertical lines in the XPS spectra. The ARPEFS curves (right) are plotted against the wave number  $k$  of the center of the corresponding integration region.

mechanisms: i.e., intrinsic in the photoemission process from the initial atomic core-electron state (as opposed, for example, to energy losses through inelastic processes extrinsic to the source atom). This conclusion stems from the extreme sensitivity of ARPEFS to the position of the outgoing elec-

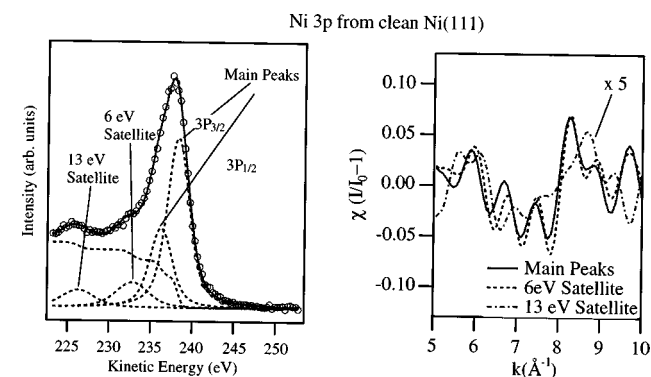


FIG. 3. Clean Ni(111) XPS spectrum (left) and normal emission ARPEFS (right). The circles in the XPS spectrum represent experimental data and the solid curve is the best fit using the components shown in dashes. The peaks were fitted with Voigt functions to extract their intensities. The main peak ARPEFS curve was derived from the sum of the  $3P^{1/2}$  and  $3P^{3/2}$  peak intensities, and it is plotted against the mean of the two main-peak positions. The 13-eV satellite curve intensity has been scaled by  $\times 5$ .

tron wave's origin, which is approximately 0.01  $\text{\AA}$ . The oscillatory ARPEFS structure in a satellite line must itself arise from interference between an unscattered outgoing wave that propagates toward the detector and an elastically scattered wave at the same kinetic energy (and  $k$  value) that scatters off neighboring atoms and then propagates toward the detector. An inelastic scattering channel would not interfere with the unscattered outgoing wave to produce an ARPEFS structure. Photoemission from a delocalized valence orbital that is not centered on an ion core would most likely lead to an outgoing electron wave that would exhibit a very different diffraction pattern.

The phenomenon of the "satellite" area of the photoemission spectrum showing ARPEFS interference structure exactly the same as that of the "main" peak can be easily understood by regarding the photoemission process as leading to eigenstates of the Hamiltonian for the core-hole manifold that are reached directly in a one-step process: the overlap of the final states and the initial ground state (exclusive of the photoemitted electron) will essentially determine the intensity spectrum for the photoemission process. Whether the spectral intensity below the main peak is discrete, as in the molecular adsorbate systems and nickel, or continuous, as in the DS line-shape case, the same general one-step picture applies.

The fact that we find these peaks to be intrinsic is compatible with the interpretation of Tillborg, Nilsson, and Martensson that the molecular adsorbate satellites are due to shakeup channels which originate from a single-step process.<sup>15</sup> This heuristic interpretation considers the final state of the remaining electrons to be strongly influenced by the newly created core hole. This state is not an eigenstate of the unperturbed system, leading to a final state that is a sum of the new eigenstates of the adsorbate-plus-core-hole system and thus has significant probability of valence excitations. The nickel 6-eV satellite is also intrinsic. This is consistent with the current understanding of its origin as being due to an excitation of a single  $d$ -level electron correlated with the  $3p$  core excitation into the continuum, leaving a  $3d^9$  valence configuration in the final state.<sup>4</sup> The DS line shape is also derived assuming an intrinsic excitation of the Fermi sea in the core-hole creation process. Our results also confirm the intrinsic origin of the DS tail. We note the relation between our results and those of Osterwalder *et al.*<sup>12</sup> who found that the plasmon-loss peaks of the aluminum 2s core level show electron scattering effects at high kinetic energies (1136 eV). At high kinetic energies, the scattering effects are dominated by forward scattering and kikuchi processes, in contrast to the energy regime of our work, which is dominated by multiple-scattering effects and backscattering.

The second conclusion that can be drawn from the similarities in the ARPEFS curves is that the transitions leading to the satellite peaks have the same values for the angular momentum variables as do those for the main peak. The dipole selection rules of photoemission are known to be valid for the main peaks and have been used successfully to model the diffraction curves for many systems. Because different angular momenta in the free-electron final state of the photoelectron lead to different and characteristic diffraction curves,<sup>22</sup> the similarity of the ARPEFS curves indicates that those angular momenta and, by implication, also the angular

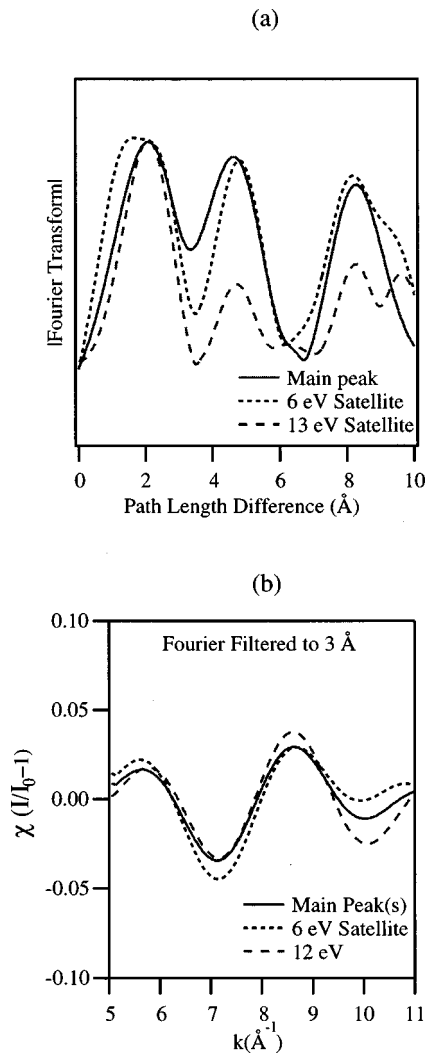


FIG. 4. (a) The Fourier transform of the nickel ARPEFS curves. (b) The ARPEFS curves, Fourier-filtered with a 3 Å cutoff to examine the phase of the dominant component. All of the 13 eV satellite curves were scaled by  $\times 5$ .

momenta of the bound, final satellite states, are the same as the angular momenta characterizing the main-peak transition.

Expressing this conclusion in the terminology often associated with discussions of satellite excitations, the valence excitations are thereby restricted to “monopole” excitations for single electrons and to a net zero angular momentum change for two-electron excitations in these systems. This agrees well with previous theoretical investigations into the 6-eV nickel satellite where a  $d$ - $d$  transition is considered the most likely origin of that satellite structure.<sup>4</sup> It has been suggested that there may be excitations to  $s$ - and  $d$ -like Rydberg states in the carbon 1s XPS of  $c(2 \times 2)$  CO/Ni(100).<sup>15</sup> However, for the similar CO/Cu(111) system, it is apparent from our data that there is essentially no angular momentum transfer and that the transitions to  $np$  states dominate.

Finally, we address the apparent difference in the nickel 13-eV satellite from the main and 6-eV peaks (see Figs. 3, 4, and 5). This peak has been attributed to the excitation of two  $d$ -band electrons at the  $3p$  resonance energy, leaving a  $3d^8$  configuration in the final state.<sup>2</sup> In Fig. 4(a) we show the Fourier transform (FT) spectrum of the three nickel ARPEFS

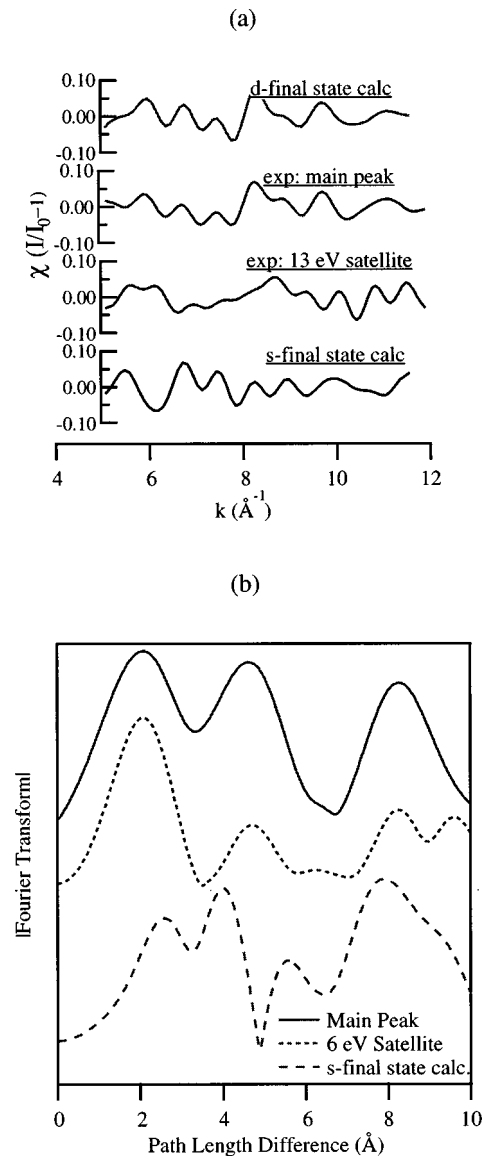


FIG. 5. Comparison of the 13-eV satellite ARPEFS curve from clean Ni(111) with  $d$ -like and  $s$ -like final-state multiple-scattering calculations and their Fourier transforms.

curves, normalized to the same intensity in the first peak. Each FT exhibits peaks at the same near-neighbor path length differences, except the 13-eV satellite peak, which shows significantly less intensity above  $\sim 3$  Å. It is not apparent from the FT whether or not the phase of the 13-eV curve matches that of the others, so we also show in Fig. 4(b) the ARPEFS curves which have been Fourier filtered to 3 Å, including only the 2 Å peak. It has been shown previously that odd-parity final states will give ARPEFS curves that are  $180^\circ$  out of phase with even-parity final states.<sup>22</sup> From the filtered curves it is apparent that the final states are of the same parity.

The angular momentum of the 13-eV satellite final state may be either  $d$  like or  $s$  like. The main peak is mostly  $d$  like, in accordance with the atomic radial matrix elements (RME) for nickel.<sup>29</sup> We have performed ARPEFS calculations using both an  $s$ -wave final state and the  $d$ -like published atomic RME.<sup>31</sup> The results of these calculations are shown in Fig. 5(a). While the  $d$ -like RME calculation

matches the main-peak ARPEFS curve very well, the  $s$ -wave curve does not. The 13-eV satellite curve does not match either calculation. The FT of the calculated and the satellite ARPEFS curves are shown in Fig. 5(b). Comparison of the satellite peak FT with the two calculations led us to conclude that the satellite peak is predominantly  $d$ -like in the final state.

We can only speculate on the suppressed intensity of oscillations of the 13-eV satellite at longer path lengths. These peaks are due to scattering from atoms more distant from the emitter than the first peak. One possible explanation is that the core hole in the presence of the  $3d^8$  configuration has a significantly shorter lifetime than the core hole with a  $3d^{10}$  or  $3d^9$  final state. This would result in a shorter coherence length of the outgoing electron wave, damping the intensity oscillations for more distant scatterers. Further theoretical investigation of the Auger decay mechanisms of the excited state would be needed to evaluate this possibility. We also considered the possibility of the peak being in some way associated with the surface of the metal. However, ARPEFS curves calculated using only the surface layer of atoms as photoemitters do not differ significantly from those of the bulk with many layers of emitters.

## V. CONCLUSION

We have shown that the photoemission satellite peaks from multielectron excitations exhibit an ARPEFS diffrac-

tion pattern. Examination of this pattern leads to unique information on the angular momentum and intrinsic/extrinsic nature of the satellite. We find that the core-level satellite peaks of carbon  $1s$  from  $(\sqrt{3} \times \sqrt{3})R30$  CO/Cu(111), nitrogen  $1s$  from  $c(2 \times 2)$  N<sub>2</sub>/Ni(100), and nickel  $3p$  from clean nickel(111) are all intrinsic peaks with final-state angular momenta identical to those for the main peaks, as dictated by the photoemission selection rules. Similarly, the tail of the Doniach-Sunjić line shapes in cobalt  $1s$  from  $p(1 \times 1)$  Co/Cu(100) and carbon  $1s$  from  $p2mg(2 \times 1)$  CO/Ni(110) also originate from intrinsic processes and have final state angular momenta identical to those for the maximum (main) peak.

## ACKNOWLEDGMENTS

We thank the staff and management of the Advanced Light Source at Lawrence Berkeley National Laboratory, the National Synchrotron Light Source and Brookhaven National Laboratory, and the Stanford Synchrotron Radiation Facility for their assistance and support with the experimental work. We also thank L. J. Terminello, L. Wang, X. Zhang, and S. Kim for their assistance with the experimental work. This work was supported by the Director, Office of Energy Research, Office of Basic Energy Sciences, Chemical Sciences Division of the U.S. Department of Energy under Contract No. DE-AC03-76SF00098.

- 
- <sup>1</sup>S. Hüfner, J. Osterwalder, T. Greber, and L. Schlapbach, *Phys. Rev. B* **42**, 7350 (1990).
- <sup>2</sup>O. Bjorholm, J. N. Andersen, C. Wigren, and A. Nilsson, *Phys. Rev. B* **41**, 10 408 (1990).
- <sup>3</sup>L. C. Davis and L. A. Feldkamp, *Phys. Rev. Lett.* **44**, 673 (1980).
- <sup>4</sup>W. Eberhardt and E. W. Plummer, *Phys. Rev. B* **21**, 3245 (1980).
- <sup>5</sup>M. Iwan, F. J. Himpsel, and D. E. Eastman, *Phys. Rev. Lett.* **43**, 1829 (1979).
- <sup>6</sup>B. W. Jepsen, F. J. Himpsel, and D. E. Eastman, *Phys. Rev. B* **26**, 4039 (1982).
- <sup>7</sup>Y. Liu, Z. Xu, and P. D. Johnson, *Phys. Rev. B* **52**, R8593 (1995).
- <sup>8</sup>N. Martensson and B. Johansson, *Phys. Rev. Lett.* **45**, 482 (1980).
- <sup>9</sup>N. Martensson, R. Nyholm, and B. Johansson, *Phys. Rev. B* **30**, 2245 (1984).
- <sup>10</sup>G. van der Laan, M. Surman, M. A. Hoyland, C. F. J. Flipse, B. T. Thole, U. Seino, H. Ogasawara, and A. Kotani, *Phys. Rev. B* **46**, 9336 (1992).
- <sup>11</sup>M. F. Lopez, A. Gutierrez, C. Laubschat, and G. Kaindl, *Solid State Commun.* **94**, 673 (1995).
- <sup>12</sup>J. Osterwalder, T. Greber, S. Hüfner, and L. Schlapbach, *Phys. Rev. B* **41**, 12 495 (1990).
- <sup>13</sup>W. F. Egelhoff, *Phys. Rev. B* **30**, 1052 (1984).
- <sup>14</sup>H. Ueba, *Phys. Rev. B* **45**, 3755 (1992).
- <sup>15</sup>H. Tillborg, A. Nilsson, and N. Martensson, *J. Electron Spectrosc. Relat. Phenom.* **62**, 73 (1993).
- <sup>16</sup>D. Lovric and B. Gumhalter, *Surf. Sci.* **278**, 108 (1992).
- <sup>17</sup>A. Nilsson, H. Tillborg, and N. Martensson, *Phys. Rev. Lett.* **67**, 1015 (1991).
- <sup>18</sup>A. Nilsson, Ph.D. thesis, Department of Physics, Uppsala University at Uppsala, Sweden, 1989.
- <sup>19</sup>J. Schirmer, G. Angonoa, S. Svensson, D. Nordfors, and U. Gelius, *J. Phys. B* **20**, 6031 (1987).
- <sup>20</sup>J. C. Fuggle, E. Umbach, D. Menzel, K. Wnadelt, and C. R. Brundle, *Solid State Commun.* **27**, 63 (1978).
- <sup>21</sup>J. J. Barton, C. C. Bahr, C. C. Robey, Z. Hussain, E. Umbach, and D. A. Shirley, *Phys. Rev. B* **34**, 3807 (1986).
- <sup>22</sup>W. R. A. Huff, Y. Zheng, Z. Hussain, and D. A. Shirley, *J. Phys. Chem.* **98**, 9182 (1994).
- <sup>23</sup>E. J. Moler, W. R. A. Huff, S. A. Kellar, Y. Zheng, E. A. Hudson, Z. Hussain, Y. Chen, and D. A. Shirley, *Phys. Rev. B* **54**, 10 862 (1996).
- <sup>24</sup>E. J. Moler, W. R. A. Huff, S. A. Kellar, Z. Hussain, Y. Chen, and D. A. Shirley, *Chem. Phys. Lett.* **264**, 504 (1997).
- <sup>25</sup>Z. Huang, Z. Hussain, W. R. A. Huff, E. J. Moler, and D. A. Shirley, *Phys. Rev. B* **48**, 1696 (1993).
- <sup>26</sup>J. A. C. Bland, D. Pescia, and R. F. Willis, *Phys. Rev. Lett.* **58**, 1244 (1987).
- <sup>27</sup>A. Clarke, G. Jennings, R. F. Willis, and P. J. Rous, *Surf. Sci.* **187**, 327 (1987).
- <sup>28</sup>J. Stohr and R. Jaeger, *Phys. Rev. B* **26**, 4111 (1982).
- <sup>29</sup>R. Raval, S. F. Parker, M. E. Pemble, P. Hollins, J. Pritchard, and M. A. Chesters, *Surf. Sci.* **203**, 353 (1988).
- <sup>30</sup>S. Doniach and M. Sunjić, *J. Phys. C* **3**, 285 (1970).
- <sup>31</sup>S. M. Goldberg, C. S. Fadley, and S. Kono, *J. Electron Spectrosc. Relat. Phenom.* **21**, 1981 (1981).